

GENERALIZED CONTROLLED SWITCHED BOND GRAPH STRUCTURES WITH APPLICATIONS TO ABRUPT FAULT MODELING

Nacusse, Matías A.^(a,b) and Junco, Sergio J.^(a)

^(a)LAC, Laboratorio de Automatización y Control, Departamento de Control, Facultad de Ciencias Exactas, Ingeniería y Agrimensura, Universidad Nacional de Rosario, Ríobamba 245 Bis – S2000EKE Rosario – Argentina.

^(b)CONICET – Consejo Nacional de Investigaciones Científicas y Técnicas.

^(a,b)nacusse@fceia.unr.edu.ar, ^(a)sjunco@fceia.unr.edu.ar

ABSTRACT

This paper presents two controlled switched Bond Graph structures with fixed causality. The first is the Switchable Structured Bond, an interconnection structure extending the idea of switchable bonds that can represent all commutation modes between two sub-systems. The second is called Generalized Switched Junction Structure and can represent all the interconnections enforced by commutations involving bond graph elements around standard 0- and 1-junctions. Both structures, defined with fixed causality for modeling and simulation purposes, can be internally represented with standard bond graph elements. To keep fixed the causality assignment even under switching, some algebraic constraints are added to the equation set of the switched structures, which in the Bond Graph domain can be represented with residual sinks. Both structures preserve causality under ideal (zero transition time) switching. Adding parasitic components as an alternative, non-ideal, approximate approach to switching can also be accomplished with the second structure just performing a minor modification on its internal implementation with basic bond graph components.

Keywords: Bond Graphs, Switched Systems, Switched Structures, Residual Sinks, Abrupt Faults.

1. INTRODUCTION

Frequently in engineering abrupt changes in physical systems are considered to occur instantaneously. This is mainly due to the fact that the behavior the engineer is interested in has a time scale much bigger than that of the abrupt change, and that the details inside the time window of this change are not relevant to the behavior under study. Thus, ignoring them results in saving time and effort. As this practice departs from the assumptions of continuity and smoothness underlying classical physics, it requires special modeling and simulation (M&S) and analysis tools to handle the systems it yields, see (Mosterman and Biswas, 1998) for a sound discussion of M&S issues related to this problem.

Bond Graphs (BG) constitutes a graphical energy-based modeling tool originally conceived to represent the continuous dynamics of physical systems (Karnopp

et al. 2000, Borutzky 2010). Many tools have been proposed in the BG domain to extend its basic component set in order to also model ideal switching processes: *MTFs modulated with gain* taking values over the set $\{0, 1\}$ (Asher 1993, Dauphin-Tanguy and Rombaut 1997); an *ideal switch* as a new bond graph element (Strömberg, Top, and Söderman 1993); a switch as an ideal current source and a voltage source (Demir and Poyraz 1997); *switchable bonds* (Broenink and Wijbrans 1993); *con-trolled junctions* (Mosterman and Biswas 1995, 1998); *Petri nets* to represent discrete modes and transition between them (Allard, Helali, Lin, and Morel 1995); and the *SPJ* or *Switched Power Junction* formalism. See (Umarikar and Umanand 2005) for an introduction to the latter modeling technique and a brief description and discussion of the pros and cons of all the others.

The results in this paper are twofold. First, after a critical review of the *switchable bond* concept (Broenink and Wijbrans 1993), a modification of it, called *S-Bonds*, is proposed. Second, it is considered how switching affects and modifies structures originally represented with elementary **0**- and **1**-junctions. The consequence of this is the introduction of two new BG components, called Generalized Switched Junction Structure (GSJ), allowing to represent all the structural changes induced by switched interconnections among the elements around the original **0**- and **1**-junctions.

Switching in a physical system can be considered under different perspectives. The research presented here was conducted in the BG-domain from a system dynamics point of view. In order to fix ideas, consider the standard state-space description $dx/dt = f(x, u; p)$, where x and u are the state- and input-vectors, and p a vector of system parameters. This model can be modified in different ways by switching, the mildest one being just a change in the values of the parameters (p -Before Switching changes into p -After Switching: $p_{BS} \rightarrow p_{AS}$) without further consequences. But more substantial modifications can occur, like changes in the vector field f defining the dynamics ($f_{BS} \rightarrow f_{AS}$) or, even more dramatic, changes in the set of state- (and/or input-) variables ($x_{BS} \rightarrow x_{AS}, u_{BS} \rightarrow u_{AS}$), with or without changes in the system order. Moreover, it could

happen that the explicit standard form be not longer attainable and substituted by a differential-algebraic system, or more generally, a differential-implicit form. All these effects are related to changes in the causality assignment if using elements of the standard BG-set, so that any tool devised to modeling switching in the BG-domain must be able to somehow address this issue.

Some M&S software do not allow changes in the causality of the model during the simulation. A possible approach to solve this is duplicating the elements with changing causality. As each of these causality-alternating, duplicated elements represents in fact a unique physical phenomenon, this modeling approach is not Object Oriented Modeling (OOM) compliant.

Also, the causal constraints at the origin of the causality switching of some elements can be broken adding some parasitic BG components, and models can be obtained with fixed causality. However these parasitic components increase the order of the model and make it stiff, which, practically, is not convenient for simulation purposes and, conceptually, enters in conflict with the ideal switch approach chosen to model the commutations. Besides this, the parasitic components are usually not related to the physical system from a macroscopic point of view, which complicates the task of parameterizing them.

Aiming at simulation with fixed causality, the causality changes are avoided in this paper following an approach already presented in (Nacusse and Junco 2010): residual sinks (Borutzky 2010) are introduced in the model to break the causality constraints produced by switching. The residual sink component injects the necessary effort or flow in order to make vanish the power conjugated variable into the sink. This bond graph component adds an algebraic constraint which implies that a DAE system describes the system dynamics. The constraint must be numerically solved at each integration step, through an explicit calculation if the constraint can be solved analytically off-line prior to the simulation, otherwise implicitly, with the consequent increment of the computational cost.

Another problem associated to the change of causality between modes is the possible appearance of discontinuities or jumps in the state trajectories, which is solved with the re-initialization of the storage elements after a switching occurrence (Nacusse and Junco 2010).

The paper is organized as follows. Section 2 presents some background results on switchable bonds, switched power junctions and residual sinks, employed in what follows. Section 3 present the Structure Switchable Bond or S_Bonds and the GSJ or Generalized Switched Junction Structures as the main results of the paper, and illustrate them with switching problems in an electric circuit. Section 4 applies the new results to two classic switched power electronic converters. Section 5 addresses the application of the GSJ structure to a fault modeling problem in a two tank hydraulic system. It is stressed that only fault modeling

is addressed and not FDI. Finally, Section 6 presents some conclusions.

2. BACKGROUND RESULTS

This section recalls the basics on SPJs, residuals sinks and switchable bonds, tools which are going to be used further in this paper.

2.1. SPJ: Switched Power Junctions

The SPJs are generalizations of the standard 0- and 1-junctions (Umarikar and Umanand 2005). They are represented as receiving the effort (0_s) or flow (1_s) information from *more than one bond*. To prevent from the causal conflicts this would otherwise imply, control signals, taking values over the set $\{1, 0\}$, are added to the new elements. Only one of these signals is allowed to have the value 1 at a given time instant, the remaining being zero. In this way, only one of the bonds imposing effort (0_s) or flow (1_s) is selected (i.e., becomes operative) and the value zero is imposed to the power co-variables of the remaining bonds, which results in their disconnection.

Figure 1 shows the SPJs with causality assignment and eqs. 1 and 2 express the mathematical relationships -for the 0_s and the 1_s , respectively- among the power variables and the control signals U_i injected to select the appropriate bond. In (Junco et al. 2007) the SPJs have been interpreted in terms of the classical 0- and 1-junctions and MTFs modulated by a gain taking the values 0 or 1. In (Nacusse et al. 2008) the implementation of the 0_s and the 1_s as new standard elements of the 20sim basic library has been presented (available at <http://www.fceia.unr.edu.ar/dsf/I&D/BG.html>).

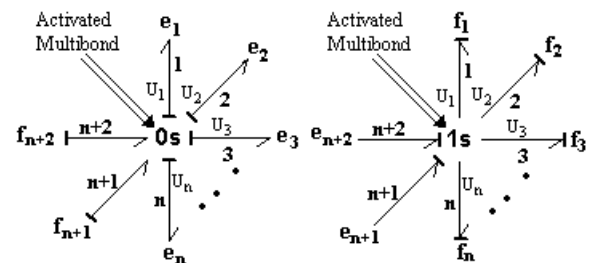


Figure 1. Switched Power Junctions with causality assignment.

$$\text{Effort} = U_1 e_1 + U_2 e_2 + \dots + U_n e_n \quad (1)$$

$$f_i = U_i (f_{n+1} + f_{n+2}) \quad ; \quad i = 1, \dots, n$$

$$\text{Flow} = U_1 f_1 + U_2 f_2 + \dots + U_n f_n \quad (2)$$

$$e_i = U_i (e_{n+1} + e_{n+2}) \quad ; \quad i = 1, \dots, n$$

The simple electrical circuit in Figure 2 illustrates how to use the SPJ technique.

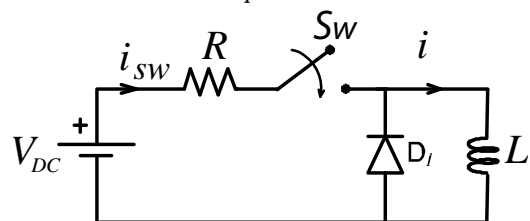


Figure 2. Switched electrical circuit

The circuit contains two switching elements, an ideal switch (an on-off commanded transistor, for instance) and a free-wheel diode, which have the complementary logic states {switch open, diode closed} and {switch closed, diode open}, so that only one control variable is necessary in the Switched BG (SwBG).

In the SwBG of Figure 3, the current commutation of the ideal switch is modeled with the 1_s and the source S_f ($f \equiv 0$), whereas the voltage commutation at the diode is modeled with the 0_s plus the resistor R labelled $D1$ (it models the diode's conduction state). Qualitatively it works as follows (consider eqs. (1) and (2) to get a more complete and precise quantitative description of this BG's behavior): the 1_s selects either the S_f -bond below it ($m=1$, switch OFF) or the bond on its right ($m=0$, switch ON) to impose, respectively, zero current or the inductance current to the submodel to its left. The 0_s chooses the $R(D1)$ -bond below it ($m=1$, switch OFF) or the bond on its left ($m=0$, switch ON) to impose, respectively, the voltage of the source-resistor series or the diode voltage-drop to the inductance. Summarizing, in this example, each SPJ chooses the bond below it ($m=1$, switch OFF) or, alternatively, both SPJs select the bond joining them ($m=0$, switch ON).

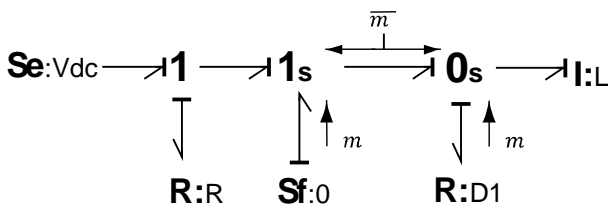


Figure 3. SwBG using SPJ of the switched circuit.

2.2. Switchable bonds

The *switchable bonds* presented in (Broenink and Wijbrans 1993) are controlled bonds commanded by a control signal m that can take the values 1 or 0 and indicates the presence or absence of the bonds in the BG model. The dashed power line indicates that this bond is only conditionally present.

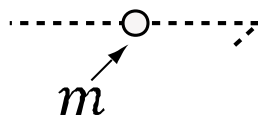


Figure 4. Switchable bond representation

This approach has some problems, caused by the fact that the boundary conditions on the adjacency of the switchable bonds are not always explicitly defined in all the switching modes (Strömberg 1994). This fact, known as the problem of the dangling junctions, is illustrated with the help of the SwBG in Figure 5, where the switches in the circuit of Figure 2 are modeled with switchable bonds. Again, the resistor R , labelled $D1$, models the diode's conduction state (note that this BG is not fully OOM-compliant, in the sense that the ideal switch, a single circuit element, has to be modeled with two switchable bonds). The problem arises when the switch is OFF and the switchable bonds commanded by

m are disconnected ($m = 0$): the source Se and the resistor R receive each an undefined flow information, each from an otherwise disconnected 1-junction. There is no problem with the switchable bond commanded by \bar{m} , which connects the I and the $R(D1)$. Also the other circuit configuration ($m = 1$) is properly defined.

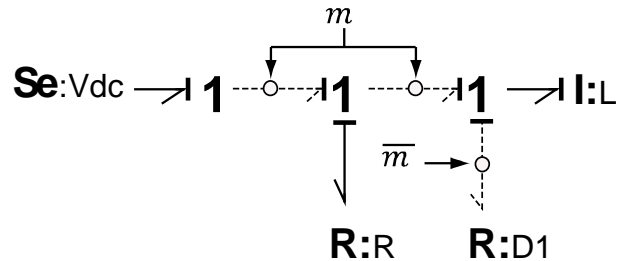


Figure 5. SwBG model of the switched electrical circuit with switchable bonds.

2.3. Residual sinks

Residual sinks are traditionally used to break causal conflicts in BG models yielding the same results as adding Lagrange multipliers (Borutzky 2010). This element injects its output variable, effort or flow, into the rest of the system, computed as to make vanish the power conjugated variable, the input into the sink.

A residual sink can be interpreted as an energy store where its parameter tends to zero. For example, an effort residual sink can be interpreted as a C element in integral causality. If the parameter C tends to zero, then \dot{e} is determined by the algebraic equation $\Delta f = 0$.

$$C \dot{e} = \Delta f \quad (3)$$

Figure 6 shows the graphical representation of the effort and flow residual sink as in (Borutzky 2009).



Figure 6. Flow and effort residual sink

3. MAIN RESULTS

The Structured Switchable Bonds, S-bonds for short, are introduced in this section as an improvement of the switchable bonds, as well as the Generalized Switched Bond Graph Structures, or GSJ, as the main contributions of the paper.

3.1. S-bonds: Structured Switchable Bonds.

The S-bonds, which can be viewed as an extension of the plain switchable bonds presented by (Broenink and Wijbrans 1993), are introduced with the aim of remedying the problem of the dangling junctions previously discussed. To do this three control signals are necessary instead of just one. Indeed, with the help of the three control variables it is possible not only to determine the presence or absence of the switchable bond, but also to explicitly and univocally define the boundary conditions of the BG-elements adjacent to the switchable bond in each switching mode. The symbology adopted is shown in Figure 7.

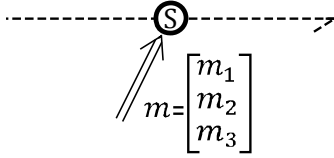


Figure 7. S-bond representation.

Without loss of generality, the behavior of the S-bond is explained with the help of Figure 8, where causality indicates that the effort e_b is imposed by Σ_a and the flow f_a is calculated by Σ_b . Besides the ground connection mode the S-bond enforces $e_b = e_a$ and $f_a = f_b$, also the switched modes must be specified where each subsystem can independently reach two modes, the zero flow (ZF) and the zero effort (ZE) mode. There are also five different operation or switching modes, which calls for three boolean-like control variables (where only 5 combinations out of the $2^3=8$ will be employed).

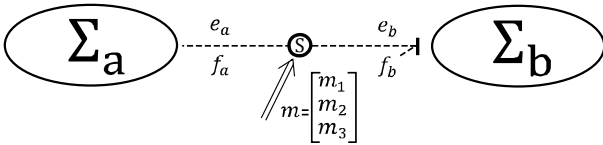


Figure 8. S-bond interconnecting two subsystems.

When Σ_b is in the ZE mode the S-bond imposes zero effort to Σ_b . On the contrary when Σ_b is in the ZF mode ($f_b = 0$) the S-bond forces the value of e_b necessary to satisfy the algebraic restriction $f_b = 0$.

When Σ_a is in the ZF mode the S-bond imposes zero flow to Σ_a . On the contrary when Σ_a is in the ZE mode ($e_a = 0$) the S-bond forces the value of f_a necessary to satisfy the algebraic restriction $e_a = 0$.

$$e_b = \begin{cases} e_a & \text{when } \Sigma_a \text{ and } \Sigma_b \text{ connected} \\ e_r & \text{when } \Sigma_b \text{ is in ZF mode} \\ 0 & \text{when } \Sigma_b \text{ is in ZE mode} \end{cases} \quad (4)$$

$$f_a = \begin{cases} f_b & \text{when } \Sigma_a \text{ and } \Sigma_b \text{ connected} \\ f_r & \text{when } \Sigma_a \text{ is in ZE mode} \\ 0 & \text{when } \Sigma_a \text{ is in ZF mode} \end{cases} \quad (5)$$

In (4) and (5) e_r and f_r are calculated through the corresponding algebraic constraints $f_b = 0$ and $e_a = 0$.

Figure 9 shows the SwBG model of the switched electric circuit of Figure 2 modeled with S-bonds. Here, each switch is represented by only one S-bond.

The S-bond commanded by m represents the electrical switch, while the S-bond commanded by \bar{m} represents the switching behaviour of the diode.

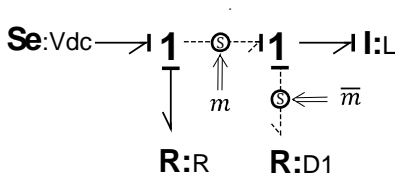


Figure 9. SwBG model of the switched electric circuit with S-bonds, $m = [m_1, m_2, m_3]$

There are no dangling junctions now: when the electric switch is OFF, the S-bond commanded by $m = [m_1, m_2, m_3]$ imposes zero flow to the 1-junction on the left and zero effort to the 1-junction on the right. At the same time, the $\mathbf{R}(D1)$ element calculates the effort imposed to the 1-junction on the right through the bond commanded by \bar{m} (the diode ON). When the switch is ON (and the diode OFF) the S-bond commanded by \bar{m} imposes zero flow to the $\mathbf{R}(D1)$ and zero effort to the 1-junction, while the other S-bond imposes the flow calculated by the I-element to the 1-junction on the left. The mathematical details of the control vector m are given in Table 1 in the next subsection.

3.1.1. Implementation of S-bonds with elementary BG components.

Figure 10 shows the internal representation of S-bonds using SPJs to model the mode switching and residual sinks to solve the algebraic constraints of each mode. The I/O relationships of this structure are given in (6) where e_r and f_r are imposed by the residual sinks. The behavior specified by Eqs. (4) and (5) is achieved with the combinations of the control variables $m_{1,2,3}$ given in Table 1.

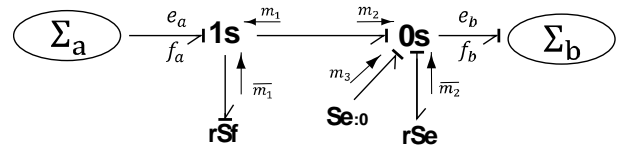


Figure 10. Internal S-bond representation

$$\begin{cases} e_b = (1 - m_3)(m_1 m_2 e_a + (1 - m_2) e_r) \\ f_a = (1 - m_3)(m_1 m_2 f_b + (1 - m_1) f_r) \end{cases} \quad (6)$$

For the sake of clarity, the model in Figure 10 uses the compact representation of SPJs and, thus, is not elementary. However, the version with BG components from the basic set can be achieved replacing the SPJs with their elementary realization as introduced in (Junco et al. 2007).

Table 1: S-bond modes and control variables.

m_3	m_2	m_1	mode
0	0	0	Σ_a in ZE and Σ_b in ZF
1	0	1	Σ_a in ZF and Σ_b in ZE
0	0	1	Σ_a and Σ_b in ZF
0	1	0	Σ_a and Σ_b in ZE
0	1	1	Σ_a and Σ_b connected

With the purpose of illustration consider the series RLC circuit of Figure 11a, where different kind of faults are expected to occur at the connection point of the resistor and the inductor, as depicted in Figs. 11b-11e. Each circuit configuration can be seen as a commutation mode between subsystems Σ_a and Σ_b . The transition among these modes and the behavior in each of them is modeled, employing S-bonds, by the SwBG of Fig. 12.

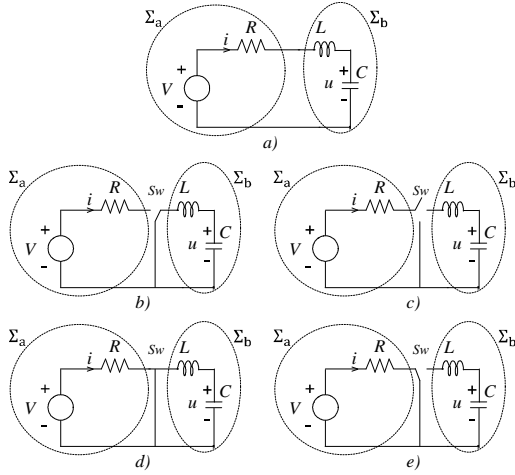


Figure 11. Series RLC circuit a) normal mode. b) Σ_a in ZF mode and Σ_b in ZE mode. c) Σ_a and Σ_b in ZF mode. d) Σ_a and Σ_b in ZE mode. e) Σ_a in ZE mode and Σ_b in ZF mode.

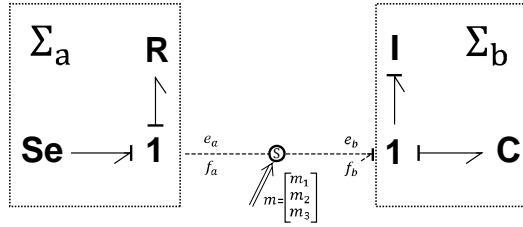


Figure 12. SwBG model of a faulty RLC circuit.

As already said, keeping fixed causality calls for the residual sinks to solve algebraic constraints in some modes. The following are the calculations of e_r and f_r for the different modes of this example. For the cases of Figs. 11c and 11e the effort on Σ_b is $e_r = e_c + \delta(t - t_c)$ where e_c is the effort of the capacitor and $\delta(t - t_c)$ is the necessary Dirac impulse of effort necessary to bring the inductance current to zero because of the switching (circuit opening) at time $t = t_c$. As in a numerical simulation the Dirac impulse cannot be implemented, to force to zero the flow in the 1-junction, the integrator of the I element must be reset to zero.

For the operation mode represented in Figure 11d, the calculus of f_r is trivial and is equal to $f_r = V/R$.

3.2. GSJ: Generalized Switched Junction Structures

The generalized switched junction structures 1-GSJ and 0-GSJ are introduced here as controlled junctions that can represent all the interconnections modes enforced by commutations involving BG-elements around the standard 0- and 1-junctions. They will be graphically represented as 0_G and 1_G .

To better understand their behavior consider that GSJ have a ground configuration where they behave like standard BG-junctions. This ground configuration is just one of their possible switching modes. In any of the other switching modes, the junction behaves as in the ground configuration but only for a subset of all the adjacent bonds, while the remaining bonds get disconnected from the junction. Thus, in a 1-GSJ (0-

GSJ) these bonds do not contribute any effort (flow) to the junction, while their flows (efforts) are determined by the structural condition which their own efforts (flows) must satisfy. The configuration of a set of control variables decides which is the subset of bonds sticking to the ground junction configuration (selected bonds) and which is the subset disconnected (not selected bonds).

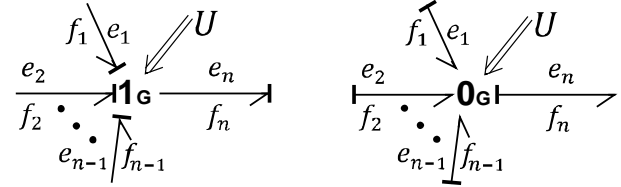


Figure 13. 1-GSJ and 0-GSJ representation

Figure 13 shows the BG iconic representation of the GSJ, where $U = [u_1, u_2, \dots, u_n]$ is the vector of control signals. In the ground configuration the bonds numbered from 1 to $(n - 1)$ impose the effort (flow) to the 1-GSJ (0-GSJ) while the n^{th} bond imposes the flow (effort) to it. Each control signal u_i ($i = 1, 2 \dots n$) can only take the value 1 or 0 and commands the i^{th} bond. In the case of the 1-GSJ, for $i = 1, 2 \dots, (n - 1)$, when u_i takes the value 0, the i^{th} bond does not contribute any effort to the junction (this does not necessarily mean that its effort is zero!). When u_n takes the value 0, then the n^{th} bond imposes zero flow (which is transmitted by the junction to the selected bonds only) and its effort is obtained from the algebraic restriction $f_n = 0$. Equations (7) and (8) specify precisely the relationships among all the variables in the 1-GSJ and the 0-GSJ, respectively.

$$\begin{cases} e_n = u_n \sum_{i=1}^{n-1} u_i e_i + (1 - u_n) e_r \\ f_i = u_i u_n f_n + (1 - u_i) f_r \quad \forall i = 1 \text{ to } n \end{cases} \quad (7)$$

$$\begin{cases} f_n = u_n \sum_{i=1}^{n-1} u_i f_i + (1 - u_n) f_r \\ e_i = u_i u_n e_n + (1 - u_i) e_r \quad \forall i = 1 \text{ to } n \end{cases} \quad (8)$$

In (7) the value of e_r is calculated through the algebraic restriction $f_n = 0$ when the 1-GSJ is in the ZF mode and the value of f_r is calculated through the algebraic restriction $\sum_{j=1}^{j=m} (1 - u_{\mu_j}) e_{\mu_j} = 0$, where $m \leq n - 1$ is the number of bonds in ZE mode and $\mu_j \in \{1, 2, \dots, n - 1\}$ (i.e., μ_j is the index of the not selected bonds). An analogue algebraic restriction is used to obtain f_r for the ZF mode of (8).

As an example of the GSJ behavior, the series circuit of Figure 11a is considered again, but in this case assuming the possible occurrence of the more ample spectrum of configurations depicted in Figures 15 and 16. All of them can be captured by the BG of Figure 14, with the control vector U defined in Table 2. There are 16 configurations in Figs. 15 and 16, the ground configuration of Fig. 16h and 15 faulty modes, so that a control vector with 4 variables is needed: $U = [u_1, u_2, u_3, u_4]$.

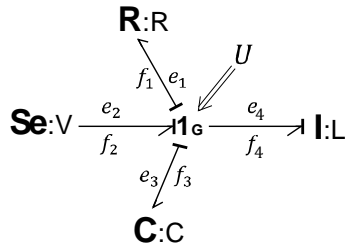


Figure 14. 1-GSJ model of switching series circuit.

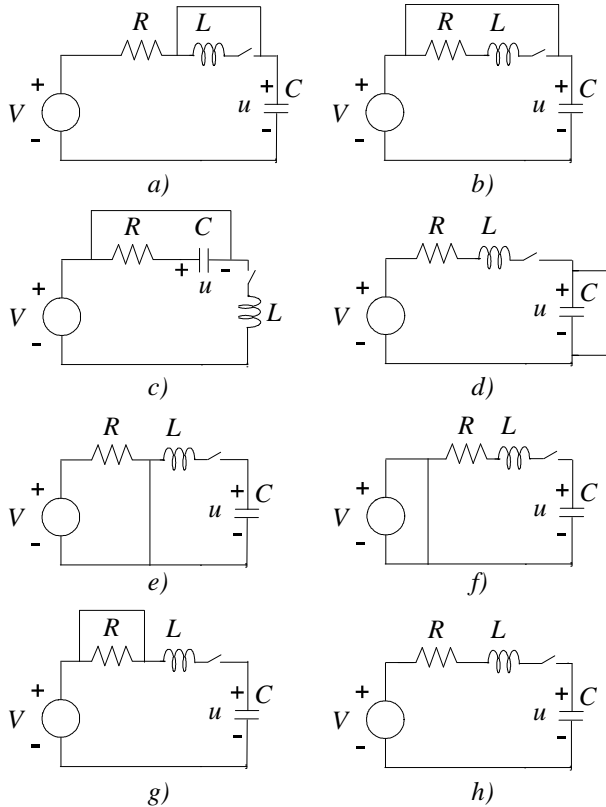


Figure 15. ZF modes of the series electrical circuit.

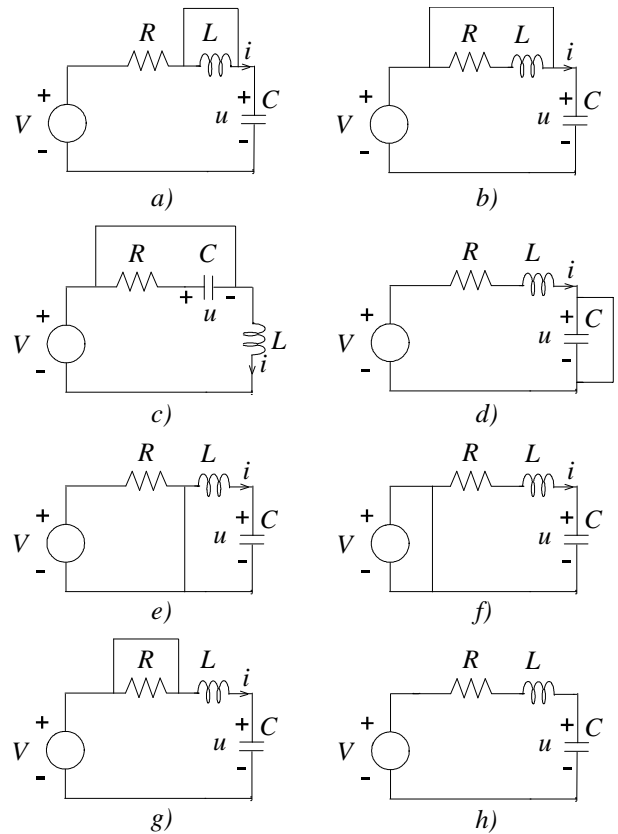


Figure 16. ZE modes of the series electrical circuit.

3.2.1. Representation of GSJ with atomic BG elements.

Following the reasoning proposed in (Junco et al. 2007) for the SPJ, also the GSJs can be represented by standards BG components as in Figures 17 and 18. The control signal enters in the BG multiplying the power variables through *MTFs*; the algebraic operations between power variables are carried out by the standard junctions of the BG formalism and the algebraic constraints are added using residual sinks.

Fig	u_4	u_3	u_2	u_1	Modes
15a	0	0	0	0	S_eRC in ZE and I in ZF
15b	0	0	0	1	S_eC in ZE and RI in ZF
15c	0	0	1	0	RC in ZE and S_eI in ZF
15d	0	0	1	1	C in ZE and S_eRI in ZF
15e	0	1	0	0	S_eR in ZE and CI in ZF
15f	0	1	0	1	S_e in ZE and RIC in ZF
15g	0	1	1	0	R in ZE and S_eCI in ZF
15h	0	1	1	1	S_eRIC in ZF
16a	1	0	0	0	S_eRIC in ZE
16b	1	0	0	1	S_eC in ZE and RI in ZE
16c	1	0	1	0	RC in ZE and S_eI in ZE
16d	1	0	1	1	C in ZE and CRI in ZE
16e	1	1	0	0	S_eR in ZE and CI in ZE
16f	1	1	0	1	S_e in ZE and RIC in ZE
16g	1	1	1	0	R in ZE and S_eCI in ZE
16h	1	1	1	1	Standard 1 – junction

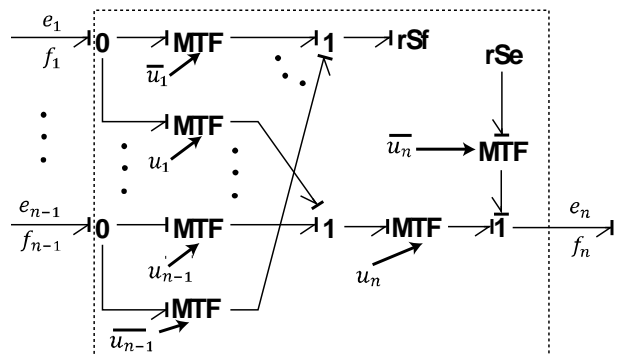


Figure 17. 1-GSJ elementary representation.

Remark: The elementary representations of Figs. 17 and 18 are also useful if the modeling approach with instantaneous commutations is resigned in favor of an approximation using parasitic components: it suffices to replace the residual sinks with the parasitic components, or with MTFs plus resistors, as done in (Borutzky 2010 and Dauphin-Tanguy and Rombaut 1997).

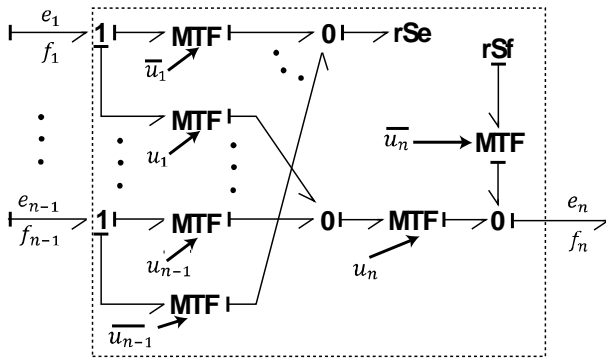


Figure 18. 0-GSJ atomic representation.

4. APPLICATION EXAMPLES: SWITCHED ELECTRONIC CIRCUITS

Modeling some switched circuits with GSJ and S-bonds, this section suggests a modeling technique.

4.1. Buck converter

The Buck converter of Figure 19 (a reducing DC-DC voltage converter: the output voltage u is less or equal than the input voltage V) contains an ideal switch (in practice, a switched transistor) and a free-wheel diode. In normal operation the diode (modeled as a resistor R , labelled DI in conduction state) and the switch have complementary logic states; in some cases, a third operation mode called discontinuous mode can take place, when the current through the diode becomes zero and both, switch and diode, are in the off state.

The basic modeling idea is to use a 0-GSJ (1-GSJ) when/where the switch commutates the application of an effort (flow) variable. In this example, the first case applies when the calculation of the potential \mathcal{P} changes according to the switch state, so that a 0-GSJ must be used to represent it. The system is modeled considering the switch closed (corresponds to the 0-GSJ in its ground state), which yields the SwBG of Figure 20, endowed with an appropriate causality assignment and the control vector $U = [u_1, u_2, u_3]$.

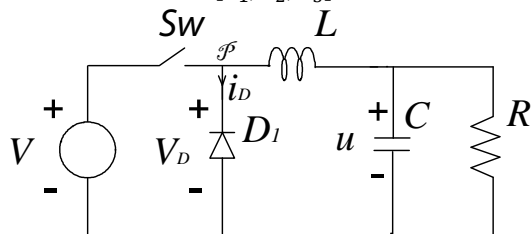


Figure 19. Schematic circuit of a Buck converter.

When the ideal switch is ON the diode is OFF $e_2 = e_3$ and e_1 is calculated through the algebraic restriction $f_1 = 0$. When the ideal switch is OFF and the diode is ON and its current i_D is less than zero (cf. the positive sense of the current i_D in Figure 19: $i_D = -f_1$), then e_2 is calculated through the algebraic restriction $f_1 - f_2 = 0$ and $f_3 = 0$. While when the diode is OFF (discontinuous operation mode of the circuit), e_2 is calculated through the algebraic restriction $f_2 = 0$. All the Buck converter operation modes are presented in Table 3.

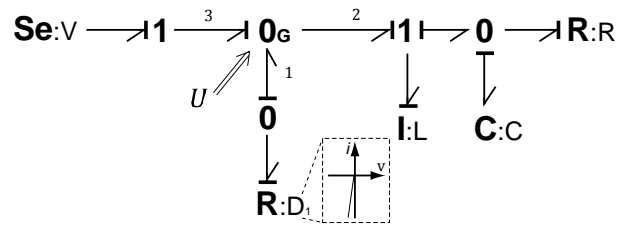


Figure 20. Buck converter SwBG model using GSJ.

Table 3: Buck converter modes

u_3	u_2	u_1	Modes
1	1	0	Switch ON, Diode OFF
0	0	0	Diode ON Switch OFF
0	1	0	Diode OFF Switch OFF

4.2. Boost converter

The Boost converter, depicted in Figure 21, is an amplifying DC-DC voltage converter, where the output voltage u is greater or equal than the input voltage V . This circuit has two operation modes, switch ON and diode OFF (mode M_1), and the opposite mode (M_2) switch OFF and diode ON. As in the previous example the diode is modeled, in conduction state, as a resistor R labelled DI .

Figure 22 shows the SwBG obtained for the Boost converter following the modeling technique suggested at the beginning of this section. It uses 1-GSJ considering that the current path is switched at node \mathcal{X} . As the diode switches its current between zero and a positive value, while the current through the inductance is always positive, the flow is imposed to the 1-GSJ by the resistor $R(DI)$. This causality assignment forces derivative causality in the inductance which is not desirable. The different operation modes of the Boost converter according to Figure 22 are reached with the control signals presented in Table 4.

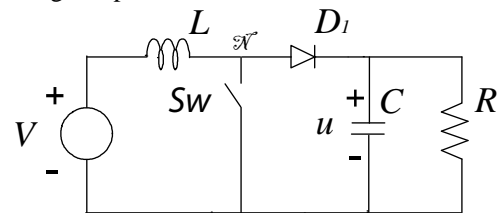


Figure 21. Schematic circuit of a Boost converter.

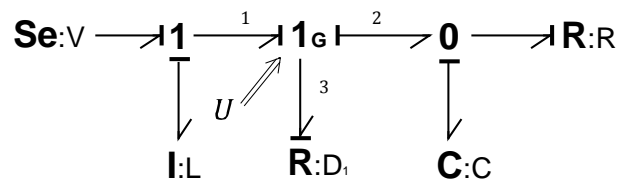


Figure 22. SwBG of the Boost converter with 1-GSJ.

Table 4: Boost converter modes of Figure 22.

u_3	u_2	u_1	modes
1	1	1	Diode ON, Switch OFF
1	0	0	Diode OFF, Switch ON

To enforce integral causality in the inductance, the 1-GSJ can be replaced by a 0-GSJ and an effort source can be placed to break the causality conflict. The resulting SwBG model is depicted in Figure 23 and Table 5 shows the different combination of the control signals to reach the operation modes.

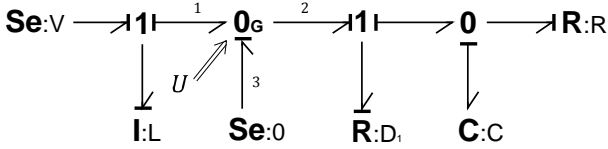


Figure 23. SwBG of the Boost converter with 0-GSJ.

Table 5: Boost converter modes of Figure 23.

u_3	u_2	u_1	modes
1	0	1	Switch ON, Diode OFF
1	0	0	Switch OFF, Diode ON

Instead of GSJs, Figure 24 uses a S-bond to model the switching in the Boost converter; its interpretation is straightforward: when the switch is ON (diode OFF) the S-bond imposes ZE to the series $S_e - I$ and ZF to the rest of the circuit. Whereas when the switch is OFF (diode ON) the S-bond works as a standard bond connecting both sub-circuits. Table 6 shows the combination of the control signals for the different configurations (cf. Eqs. 6).

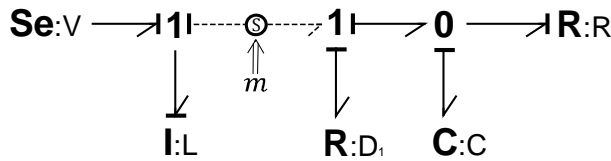


Figure 24. SwBG of the Boost converter with S-Bonds.

Table 6: Boost converter modes with S-bonds

m_3	m_2	m_1	modes
0	0	0	Switch ON, Diode OFF
0	1	1	Switch OFF, Diode ON

5. APPLICATION TO FAULT MODELING: FAULTY TWO TANK SYSTEM.

The application example consists in two tanks separated by a distance $L = L_1 + L_2$ and connected by two pipes and a valve (V_{12}) which controls the flow passage as shown in Figure 25. The pipe 1 connects the Tank1 with the valve V_{12} and has a length L_1 , while pipe 2 connects the valve V_{12} with the Tank2 and has a length L_2 . Figure 26 shows the associated BG model.

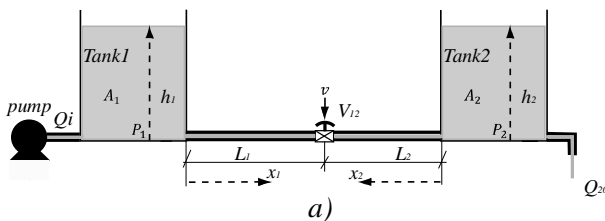


Figure 25. Two tanks physical system.

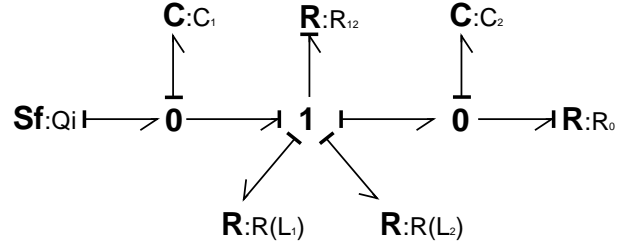


Figure 26. BG model of healthy two tank system.

The following constitutive relationships of the BG elements of Figure 26 are assumed: $R(x_i): Q = \frac{a_i}{x_i + D} \sqrt{\Delta P} \text{sign}(\Delta P)$ where a_i and x_i (with $i = 1, 2$) represents the cross section and length of the pipes while D match the value of the restriction when $x_i = 0$; $R_{12}: Q = a_{12} v \sqrt{\Delta P} \text{sign}(\Delta P)$ where a_{12} is the discharge coefficient of the valve and v is the opening control of the valve; $R_0: Q = a_0 \sqrt{\Delta P} \text{sign}(\Delta P)$ where a_0 represents the cross section of outlet hole from Tank2; $C_i = \frac{A_i}{\rho g}$ (with $i=1,2$) are the tanks hydraulic capacities where A_1 and A_2 are the cross section areas of the tanks ρ is the constant density of the liquid, g is the gravitational acceleration.

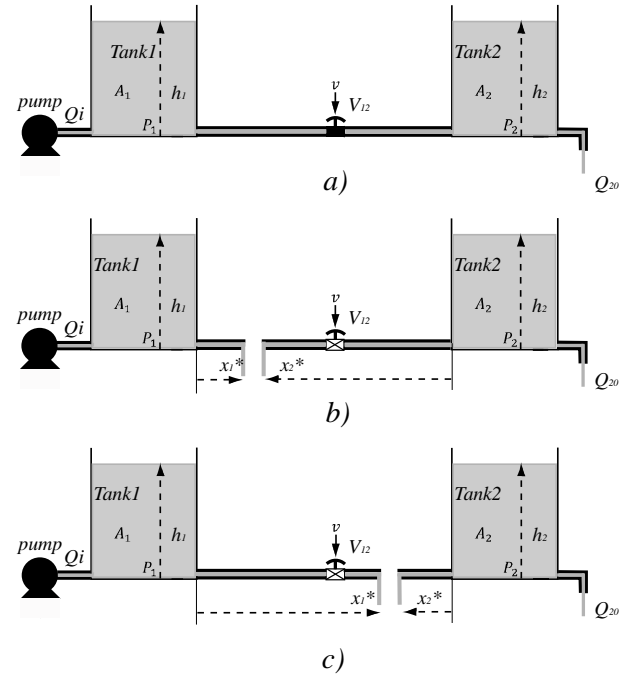


Figure 27. Fault modes of the two tank system. a) Valve V_{12} blocked, b) broken pipe at x_1^* , c) broken pipe at x_2^* .

In this example three different abrupt faults are considered for modeling purposes, as shown in Figures 27a,b,c. The first one is a blockage in the valve V_{12} , the second and the third one corresponds to the pipe broken at position x_1^* and x_2^* respectively. All these faults break the shared flow constraint of the pipes and the valve. So, to represent the structural changes produced by the faults a 1-GSJ can be placed instead of the standard 1-junction, which yields the SwBG model of Figure 28.

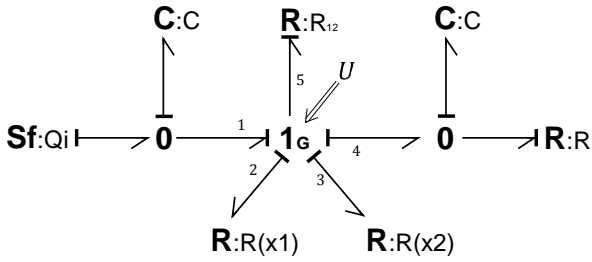


Figure 28. SwBG model of the faulty two tank system.

Table 7 shows the combinations of the control signals that generate the healthy and the faulty modes. Figures 29, 30, 31 explicitly show, in the form of BG models, the different calculations implemented by the 1-GSJ in the faulty modes as determined by the signals of the control vector $U = [u_1, u_2, u_3, u_4, u_5]$.

Table 7: two tank modes

u_5	u_4	u_3	u_2	u_1	Two tank process modes
1	1	1	1	1	Healthy
1	0	0	1	1	Pipe 2 broken at x_2^* .
1	1	1	0	0	Pipe 1 broken at x_1^* .
0	1	1	1	1	Valve V_{12} blocked (ZF mode)

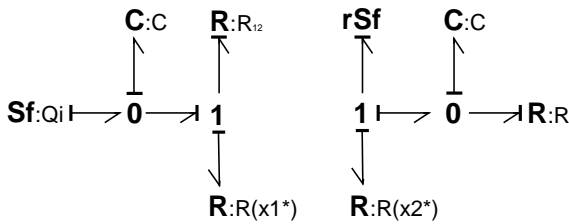


Figure 29. Pipe 2 broken at x_2^* , $U = [1, 1, 0, 0, 1]$

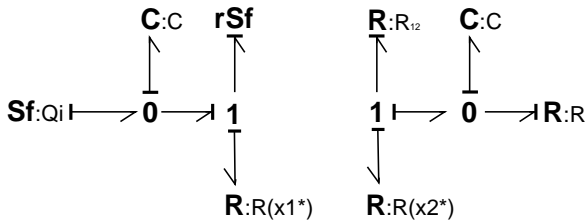


Figure 30. Pipe 1 broken at x_1^* , $U = [0, 0, 1, 1, 1]$.

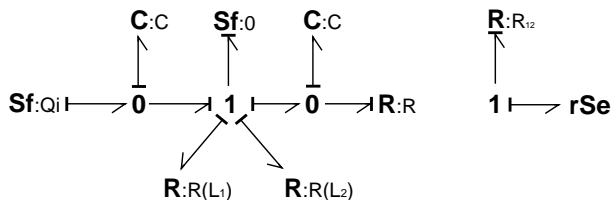


Figure 31. Valve V_{12} blocked, $U = [1, 1, 1, 1, 0]$

5.1. Simulation results.

In this subsection some simulation results are presented to show the correct behavior of the GSJs.

The following parameters are used in the simulations (Samantaray and Ould Bouamama 2008): $A_i = 1.45 \cdot 10^{-2} m^2$, $a_{12} = 1.593 \cdot 10^{-2} kg^{1/2}m^{1/2}$, $Q_i =$

$1 m^3/s$, $L_1 = 1m$, $a_0 = 1.596 \cdot 10^{-2} kg^{1/2}m^{1/2}$, $L_2 = 1 m$ and $a_i = 0.03 kg^{1/2}m^{1/2}$, $D = 0m$, $v = 1$.

In all simulation responses from top to bottom, P_1 is the pressure at the bottom of Tank1 in N/m^2 , P_2 is the pressure at the bottom of Tank2 in N/m^2 , Q_{1out} is the output mass flow of Tank1 in m^3 , Q_{2in} is the input flow mass of Tank2 in m^3 and Q_{2out} is the output flow mass of Tank2 in m^3 .

Figure 32 shows the simulation response of a fault in the pipe that connects Tank1 with the valve V_{12} . The fault occurs at time $T = 310 s$ and at a distance $x_1^* = 0.5 m$, which implies that $x_2^* = 1.5 m$.

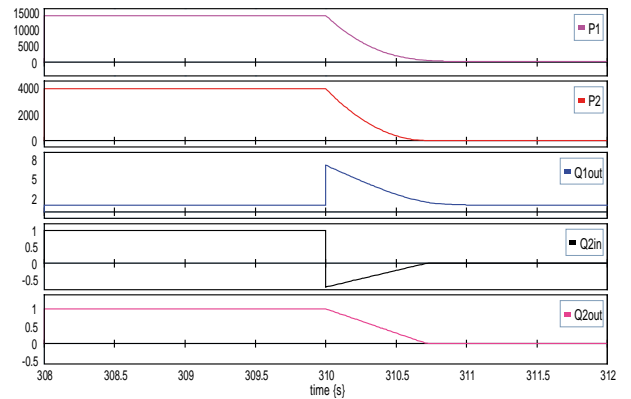


Figure 32. Simulation response with pipe 1 broken at x_1^* .

Figure 33 shows the simulation response of a fault in the pipe that connects Tank2 with the valve V_{12} . The fault occurs at time $T = 310 s$ and at a distance $x_2^* = 0.5 m$ which implies that $x_1^* = 1.5 m$.

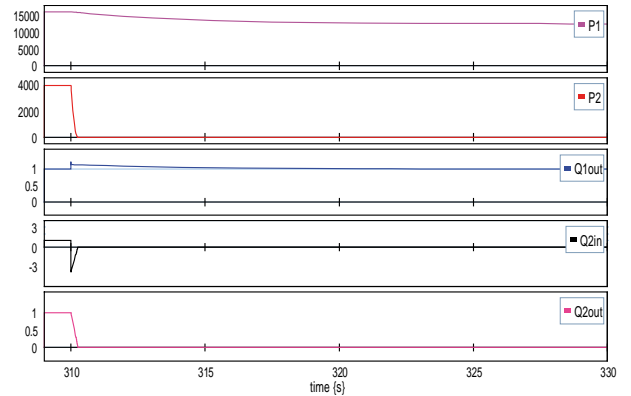


Figure 33. Simulation response with pipe 2 broken at x_2^* .

To perform a simulation of sequential structural faults, the control signal U starts with $U = [1, 1, 1, 1, 1]$ (system in healthy mode), then changes to $U = [0, 1, 1, 1, 1]$ (commutation to “valve blocked”) and, finally, switches to $U = [0, 1, 1, 0, 0]$ (“valve blocked and pipe 1 broken at x_1^* ”). Notice that the latter faulty mode is not in Table 7. Figure 34 shows the simulation response of this sequence of structural faults. At $T = 300 s$ the valve V_{12} gets blocked; then, pipe 1 breaks at $T = 302 s$ at $x_1^* = 0.5 m$.

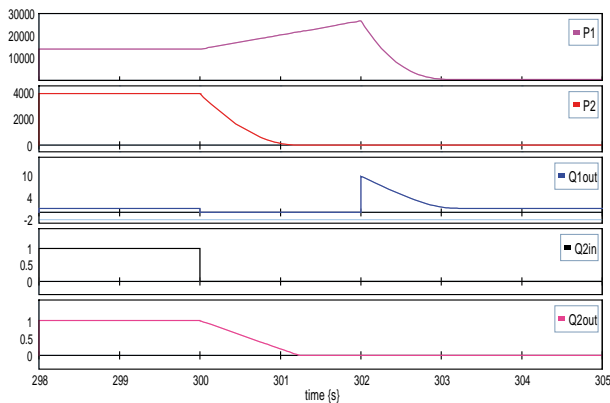


Figure 34. Simulation response with sequential faults.

6. CONCLUSIONS

This paper introduced two new fixed-causality formalisms to handle ideal switching processes -i.e., commutations happening within a null time span- in the Bond Graph domain. The first one, called Switchable Structured Bond, S-Bond for short, allows to model the power connection/ disconnection (presence/absence of a bond) between two subsystems and, at the same time, solves the “dangling junction” problem known to happen in the classical switchable bonds. The second one, called GSJ for Generalized Switched Junction Structure, allows to represent the classical structure of a standard BG-junction (called the ground configuration of the GSJ) *plus* all possible commutations involving the elements joined by the structure in its ground configuration. Both, a macro definition or representation and an internal implementation with elementary BG-components are provided for each of the new structures. A minor modification of the GSJ internal representation allows to alternatively adopt an approximate approach to switching modeling with the use of parasitic components. A procedure to construct the switched bond graphs models using these new techniques has been suggested. Also, application examples of controlled and fault-induced switching have been provided, together with some simulation results in the latter case.

ACKNOWLEDGMENTS

The authors wish to thank CONICET (the Argentine National Council for Scientific and Technological Research), and SeCyT-UNR (the Secretary for Science and Technology of the National University of Rosario) and PICT 0650-2008 for their financial support.

REFERENCES

Allard, B., Helali, H., Lin, Ch., Morel, H., 1995. Power converter average model computation using the bond graph and Petri Net Techniques. *IEEE Power Electronic Specialist Conference*, pp. 830–836.

Asher, G., 1993. The robust modeling of variable topology circuits using bond graphs. *Proc. ICBGM'93, the Int. Conf. on Bond Graph Modeling and Simulation*. pp. 126–131. San Diego, CA.

Borutzky, W., 2010. *Bond Graphs. A Methodology for Modelling Multidisciplinary Dynamic Systems*. Erlangen, San Diego: SCS Publishing House.

Borutzky, W., 2009. Bond graph model-based fault detection using residual sinks. *Proc. IMechE, Part I: Journal of Systems and Control Engineering*, Vol. 223, London: PEP. pp. 337-352.

Broenink, J. and Wijbrans, K., 1993. Describing discontinuities in bond graphs. *Proceedings ICBGM'93*. pp. 120–125 San Diego, CA.

Dauphin-Tanguy, G. and Rombaut, C., 1997. A Bond Graph Approach For Modeling Switching Losses of Power Semiconductor Devices. *Proc. ICBGM'97*. pp. 207-212. Phoenix, Arizona, USA.

Demir, Y. and Poyraz, M., 1997. Derivation of state and output equations for systems containing switches and a novel definition of switch using the bond graph model. *J. Franklin Institute*. 334 (2) 191–197.

Lin, H. and Antsaklis, P., 2007. Switching Stabilizability for Continuous-Time Uncertain Switched Linear Systems. *IEEE TAC*. Vol. 52, N°4. pp 633-646.

Junco, S., Diéguez, G., Ramírez, F., 2007. On commutation modeling in Bond Graphs, *Proc. Int. Conf. on Bond Graph Modeling and Simulation*, pp. 12-19. San Diego, CA.

Karnopp, D., Margolis, D., Rosenberg, R., 2000. *System Dynamics. Modeling and simulation of mechatronic systems*, 3rd edition, Wiley Inter-science, New York.

Mosterman, P. and Biswas, G., 1995. Behaviour generation using model switching. A hybrid bond graph modeling technique. *Proc. ICBGM'95*. pp. 177–182. Las Vegas, USA.

Mosterman, P. and Biswas, G., 1998. A theory of discontinuities in physical systems models. *Journal of the Franklin Institute*, 335B (3), 401–439.

Nacusse, M., Junco, S., Donaire, A., 2008. Automatizando el Modelado y Simulación con Bond Graph de sistemas Físicos Computados. *Mecánica Computacional*. XXVII, pp. 3479-3494.

Nacusse, M., Junco, S. 2010. Automatic handling of commutations in Bond Graph based Simulation of Switched Systems. *Proc. 4th Int. Conf. on Integrated Modeling and Analysis in Applied Control and Automation (IMAACA2010)*. pp. 27-35. Fes, Morocco.

Strömberg, J., Top, J., Söderman, U., 1993. Variable causality in bond graph caused by discrete effects. *Proc. Int. Conf. on Bond Graph Modeling and Simulation*, pp. 115–119. San Diego, CA.,

Strömberg, J. E. 1994. *A mode switching modelling philosophy*. Phd Thesis, Department of Electrical Engineering. Linköping University, Sweden.

Samantaray, A.K., Ould Bouamama ,B. 2008. *Model-based Process Supervision*. Springer Verlag London Ltd.

Umarikar, A. and Umanand, L., 2005. Modelling of switching systems in bond graphs using the concept of switched power junctions. *Journal of the Franklin Institute*, Vol. 342, pp. 131-147.